A Biologically Degradable and Bioseniatic™ Feedstock for the High-Quality 3D Printing of Anatomical Models

Joshua C. Bledsoe, Brad E. Gilleland, Austin F. Wright, Evan M. White, Grant H. Crane, Christopher B. Herron, Jason J. Locklin, and Branson W. Ritchie

A Poly(3-hydroxybutyrate-co-3-hydroxyhexanoate) (PHBHHx) -based filament was evaluated as an alternative feedstock for Fused Deposition Modeling (FDM) of instructional and clinical medical specimens. PHBHHx-based prints of domestic cat vertebrae, skull bone, and an aortic arch cast were found comparable to conventional materials. PHBHHx-based filament and extrudate samples were evaluated for biological degradability, to meet the Bioseniatic™ standard, defined by the University of Georgia New Materials Institute. Both samples achieved more than 90% mineralization within 32 days in industrial composting conditions.

Keywords

3-Dimensional (3D) printing, biological degradability, Bioseniatic™, educational, fused deposition modeling (FDM), anatomical models, polyhydroxyalkanoate (PHA)

Introduction

Among the more than 12 types of 3-Dimensional (3D) printing technologies, fused deposition modeling (FDM) is the simplest, most user-friendly, and least toxic method. FDM was originally patented in 1989 by S. Scott Crump (Crump 1992), who then created Stratasys, a now well-renowned manufacturer and seller of 3D printers and 3D printed parts. Through technology and manufacturing advances, different forms of 3D printing have revolutionized medical modeling, facilitating quick and high-quality production (Paul et al. 2018, Low et al. 2019, Squelch 2018, Yap et al. 2017, George et al. 2017). The most common FDM feedstock materials include polylactic acid (PLA), acrylonitrile-butadiene-styrene (ABS) copolymer, and polyethylene terephthalate glycol-modified (PETG). Most FDM waste ends up in landfills (managed waste) or as mismanaged waste in our oceans, lakes, and lands where it degrades through micronization into environmentally persistent and ecologically damaging particles. Additionally, unaware consumers may attempt to recycle common 3D printing wastes with other household recycling, where the non-recyclable 3D filament compounds contaminate recyclable plastics, often leading to recycler rejection of the plastics which are then sent to a landfill. Currently, the only readily available alternative to environmentally persistent FDM materials is PLA or PLA/ polyhydroxyalkanoates (PHA) blends, which are industrially compostable, but not biologically degradable in other field conditions. Further, PLA is being increasingly scrutinized as an alternative to environmentally persistent plastics because it degrades much more slowly than common industrial compostable organics (i.e., food waste, green waste, etc.) resulting in additional expenses from the reduced frequency of compost harvesting. As a result, PLA is now commonly rejected from composting facilities. Regardless of the polymer used or the type of printer used, mismanaged 3D printing waste contributes to the plastic pollution crisis of today, and the impact of 3D printing waste is expected to proliferate exponentially as 3D printing continues to increase in popularity in coming years (Rodríguez-Hernández et al. 2020). Scientific research on the ecological and health (plasticosis) impacts of micronization of non-biologically degradable materials has reached a renaissance with the recognition that plastic pollution has become a global crisis (White et al. 2018, Lavers 2019, Ritchie 2022) that will continue to intensify, before environmentally persistent plastics can be replaced with biologically degradable alternatives. Better options for FDM feedstocks are needed to prevent the already intractable problem of plastic pollution from progressing due to 3D printing wastes.

PHAs are a class of bio-polyesters which are produced as an energy and carbon storage mechanism in bacteria. The chemical structures of individual PHAs can vary widely, but most commonly include 3-hydroxybutyric acid (3HB) as a repeating unit. Specific modification of the fermentation feedstocks allows for the selective copolymerization of 3HB with any of a series of over 150 comonomers, affording the broader set of tunable PHA copolymers (Chen 2010). The comonomers in PHAs are generally categorized according to their side-chain length, which impacts their processability and overall materials properties. PHAs in general are becoming increasingly available as manufacturers increase production capacity. The 3D printing of PHAs has been investigated in recent publications, focusing on stereolithography (SLA), selective laser sintering (SLS), and FDM of neat materials, in addition to commercially available blends of PLA and PHA (Mehrpouya et al. 2021, Gregory et al. 2023). Poly(hydroxybutyrate-*co*-hydroxyhexanoate) (PHBHHx), a copolymer containing 3-hydroxyhexanoic acid (3HHx), has been investigated in the formation of 3D scaffolds, but has not been evaluated for the

production of high-quality anatomical models (Kovalcik et al. 2020). Given the historic and continued growth of FDM printing in the hobbyist and industrial markets, an alternative FDM feedstock formulated from specific PHA-based polymers could provide an environmentally friendly biologically degradable alternative to environmentally persistent FDM. Additionally, PHBHHx is a semicrystalline polymer (Qu et al. 2005) whose resistances to environmental factors, while in use, are expected to be similar to those of PLA, due to their similar structures (aliphatic polyesters). Therefore, the present work evaluates the performance of a new PHBHHx-based FDM feedstock developed by the UGA New Materials Institute, identified as "NMI filament", and verifies its biological degradability that meets the Bioseniatic™ standard defined by the New Materials Institute at the University of Georgia (University of Georgia n.d. 2020). The Bioseniatic™ criteria require greater than 90% conversion to biogases, water, or non-toxic compounds within a reasonable time in simulated managed or mismanaged environments. The present research evaluated the biological degradation, disintegration, and toxicity of the PHBHHx-based feedstock.

Methodology

Materials

PHBHHx copolymer filament (NMI filament) was toll manufactured from polymer produced by the New Materials Institute (Athens, Georgia). The filament was used as supplied, and maintained exceptional diameter tolerance (1.75 ± 0.01 mm). White PLA FDM filament, 1.75mm diameter was purchased from Hatchbox (Pomona, California, USA) and was used without modification. White SLA resin was purchased from Formlabs (Sommerville, Massachusetts, USA) and was used without modification.

FDM 3D Printing

Medical illustration (.stl) files for each print were loaded into Ultimaker Cura (Ver. 4.11.0) slicing software and converted into printing instruction (.gcode) files. Unless otherwise specified (Supplementary Appendix), the print settings were the default values of the “Generic PLA” material setting and the default “Standard Quality – 0.2mm” print profile. .gcode files were loaded onto an Creality Ender 3 (Shenzhen, China) for printing. A thin coat of build plate adhesive (Magigoo) was applied to discourage print delamination.

SLA 3D Printing

.stl files were loaded into PreForm (Ver. 3.2.8) slicing software and converted into .gcode files. The print settings were the default values of the “White Material” setting and the fastest “Layer Thickness – 0.100 mm” print profile. .gcode files were loaded into a Formlabs Form 2 for printing.

Post-Processing of Printed Articles

FDM printed PLA and NMI filament samples were manually removed from their build plates. Support structures were removed using pliers and snippers. SLA printed samples were washed in a Form Wash print washing unit (Formlabs) for 10 minutes using 91% isopropanol as a washing solution. After drying at room temperature, the prints were post-cured using a Form Cure unit (Formlabs) for 30 minutes at 60°C. SLA supports were removed manually using pliers and snippers.

Respirometry

Samples were investigated for biological degradation under modified conditions outlined in ASTM D5338 – 15 under industrial composting criteria. Mature compost, aged approximately 2 – 4 months, was sourced from two separate industrial composting facilities, averaging 46±5°C at sourcing locations 30 – 100 cm in depth. The compost was then particle sieved through a 4.76 mm screen and adjusted to a pH of 7.10 using gypsum with 14% w/w sulfur (**Table S1**). The two samples of separately sourced compost were then blended in a 50:50 mass ratio to increase the microbiological diversity of the test inoculum. The compost was stored at room temperature prior to respirometry analysis. The inoculum was analyzed for the concentrations of various metals through total acid digestion (**Table S2**). The compost inoculum was measured directly prior to testing to have a pH of 7.19, a total solids content of 50.60%, and a total volatile solids content of 53.49%. Each test consisted of 6 grams of test material or positive control being introduced to 250 grams of inoculum prepared in a contained 2.7-liter bioreactor with a refillable water reservoir. The blank control used only 250 grams of inoculum prepared in a bioreactor. All sample and control groups were studied in triplicates at 58±2°C to ensure statistical accuracy and reproducibility. All respirometers and hardware are maintained daily. Reactor contents are stirred weekly. Moisture content from all reactors is analyzed weekly. Clean, deionized water may be added as necessary to a reactor’s reservoir or inoculum to keep the moisture of the inoculum between 45-60%.

Disintegration Photography

The compost inoculum prepared for respirometry was used for disintegration testing. Approximately 1.5 kilograms of compost was added to a polypropylene container with two 3 mm air holes on opposite sides of the box, just above the inoculum surface. Samples of filament were cut to length and incubated in the compost at 58°C. Photographic images of the samples were taken approximately once every two weeks and samples were replaced into the compost.

Raman microscopy

After respirometry studies, residues from the triplicate samples were combined and mixed well. Small aliquots of compost residues (about ~7500 particles) were surveyed by microscopy to identify any filament sample residues. A sample set of several hundred particles were targeted by Raman microscopy

to identify any Raman spectra that match the original sample spectrum (**Figures S4 – S6**). An internal control of polystyrene microbeads was deposited onto the quartz slide and used to analyze the compost residues to ensure particle targeting and Raman spectra fidelity.

Toxicology Studies

To model the ecotoxicity of PHA as it degrades, an earthworm, *Eisenia fetida*, was selected as a model organism and toxicology analysis was examined according to ASTM E1676 – 12 methods. Twelve glass mason jars (16-oz) were filled with 200 grams of naturally sourced soil (from the UGArden on campus in Athens, GA) at approximately 30% moisture and were topped with pierced parafilm. Soil properties and chemicals were analyzed prior to testing in collaboration with the UGA Soil Laboratory. Six of the jars remained untreated as a control set. Cryoground test PHBHHx filament was introduced to soil in two different concentrations: Three jars received 0.6 grams (4,300ppm) of the NMI filament, and three jars received 6.74 grams (48,000ppm) of the NMI filament.

Ten adult worms approximately 2.5 cm in length or greater were selected to stock the testing vessels. Once introduced, the organisms were left undisturbed for two weeks and exposed to a 12-hour light dark cycle in a controlled climate environment. The vessels were provided with positive airflow. Total population count and total organismal biomass per vessel was compared before and after the study. Moisture and pH measurements are taken before and after the study.

Filament Water Absorption Study

10.0 ± 0.5 grams of PHBHHx copolymer and PLA filaments were submerged in municipal water and stored under ambient conditions for 1 month. Filament samples were periodically removed and gently patted dry before weighing to determine the increase in mass due to absorbed water. Weighed samples were then resubmerged in water and testing was resumed.

Results

Printability Study of Anatomical Models Using NMI Filament

Printability was first evaluated on "medium-sized" models consisting of a malformed domestic cat skull (**Figure 1**) and an aortic artery (**Figure 2**) in comparison to a standard PLA print. Printing parameters for the medium-sized prints are shown in (**Table 1)**. Printing parameters were chosen to optimize polymer flowability during print, while limiting unnecessary molecular weight reduction of printed specimens by exposure to temperatures above thermal degradation onset ($T_{deg,\ PHBHHx}$).

Table 1. Print parameters for medium-sized FDM prints.

Print Setting	Value
Nozzle Temperature	212°C
Build Plate Temperature	84°C
Print Speed	35 mm/s

In cat skull printing, NMI filament performed similarly to PLA but exhibited improved surface texture. NMI filament support structures were more difficult to remove than PLA, due to the greater ductility of the PHBHHx copolymer. As a result, support structures within the sinus passages and eye socket of the NMI filament print were not fully removed.

Figure 1. FDM prints of a deformed domestic cat skull using PLA- (left) and PHBHHx- (right) based filaments.

Based on the extensive 3D printing experience of the medical illustrator author, NMI filament performed similarly to PLA in aortic artery printing. Slight banding along the NMI filament print was visible due to the lack of opacifiers in the filament. In this case the additional strength of NMI filament prints made handling them easier, compared to typically fragile PLA FDM prints. Breaking of PLA FDM prints during post-processing is common but was considered less likely with the more ductile NMI filament used for printing these models.

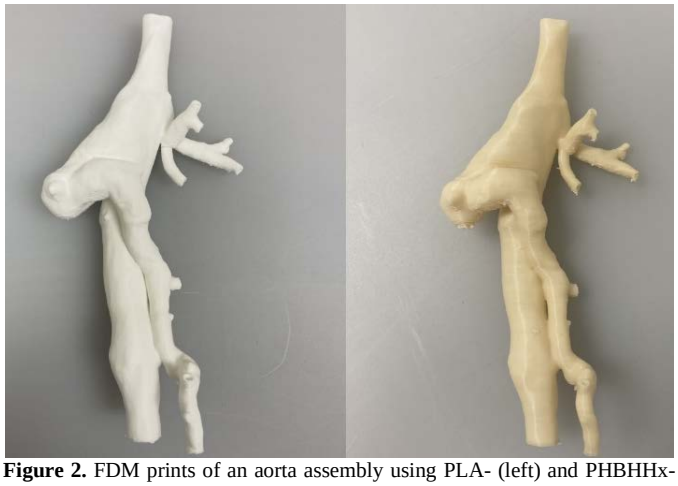

Figure 2. FDM prints of an aorta assembly using PLA- (left) and PHBHHx- (right) based filaments.

Printability of NMI filament was expanded to smaller, more detailed anatomical models. On initial comparison, the print parameters for the medium-sized prints were insufficient for high-quality printing (**Figure 3**) of smaller models due to an excess of stringing, defects, and geometric instability. The printing parameters for the NMI filament were adjusted to accommodate the enhanced precision needed for high quality printing of small articles (**Table 2**). Print temperature was reduced to 205°C to reduce the viscosity during printing, resulting in improved geometric stability, and print speed reduction from 35 mm/s to 15 mm/s provided more crystallization time per layer, improving print resolution in the z-axis. The decrease in build plate temperature was not expected to have substantially improved printability, however decreasing build plate temperature was beneficial by reducing the overall power consumption of the printing process, further supporting the environmental friendliness of the NMI filament. The resulting printability of small articles was enhanced and became more closely comparable with the standard SLA prints (**Figure 4**). SLA is typically chosen for small prints due to the increased precision and surface quality afforded by low print layer height. The decrease in print speed for small prints was expected to result in an increased print time. The print times range from 58 minutes when both vertebrae are printed together at 35 mm/s to 82 minutes at 15 mm/s, a 41% increase in time for the slower print. However, the improved print quality at this slower rate appeared favorable, and any waste NMI filament and resulting prints would be biologically degradable. As a final means of comparative analysis, the water absorption rates of the NMI and PLA filaments were determined after submersion for one month in municipal water. The NMI and PLA filaments performed similarly, absorbing less than 1 w/w% of water over the assessed period (NMI Filament: 0.9 w/w%, PLA: 0.7 w/w%). A table of the water absorption rate with respect to time is provided in the Supplementary Appendix (**Table S3**).

Figure 3. Imperfect print quality in PHBHHx- (right) based filament printing of small parts due to improper print parameter optimization, in comparison to standard SLA prints (left).

Table 2. Print parameters for small-sized FDM prints.

Print Setting	Value
Nozzle Temperature	205°C
Build Plate Temperature	Ambient (25°C)
Print Speed	15 mm/s

Figure 4. Improved PHBHHx- (right) based filament print quality of vertebrae samples, compared to standard SLA prints (left).

The biologic degradation performance of the NMI filament was investigated by means of respirometry, disintegration, Raman microscopy, and toxicological studies. Given the tendency for thermal degradation of PHBHHx upon heating, non-printed filament samples and extrudates formed by melting the filament through the 3D printing nozzle were separately investigated. These test samples simulate how waste filament, as well as any print made from the filament, would degrade in industrial composting conditions. The NMI filament and extrudate samples degraded rapidly under industrial compost conditions, achieving >90% degradation, as measured by carbon mineralization in the respirometer after 27 and 32 days, respectively (**Figure 5a**). In comparison to cellulose, a positive control, the NMI filament samples showed slower initial biodegradation, but achieved an overall higher level of biologic degradation. The absolute biodegradation of cellulose was only 71.5% at 39 days, which was lower than the expected value of 100%, as cellulose is a highly degradable natural material. The lower biodegradability in this case is likely due to a somewhat poorly active compost. A separate evaluation revealed an unusually high ammonia content (the compost mix for this experiment was measured at 2,798 mg/kg ammonia, higher than historical averages near 150 mg/kg from these sources) which likely raised the pH of the compost, reducing microbial catabolism of cellulose. Despite sub-optimal industrial compost conditions, NMI filament and extrudate samples were rapidly catabolized in industrial composting conditions (**Figure 5b**). Raw cumulative CO_2 captured from biodegradation reactors is available in the Supplementary Appendix (**Figure S1**).

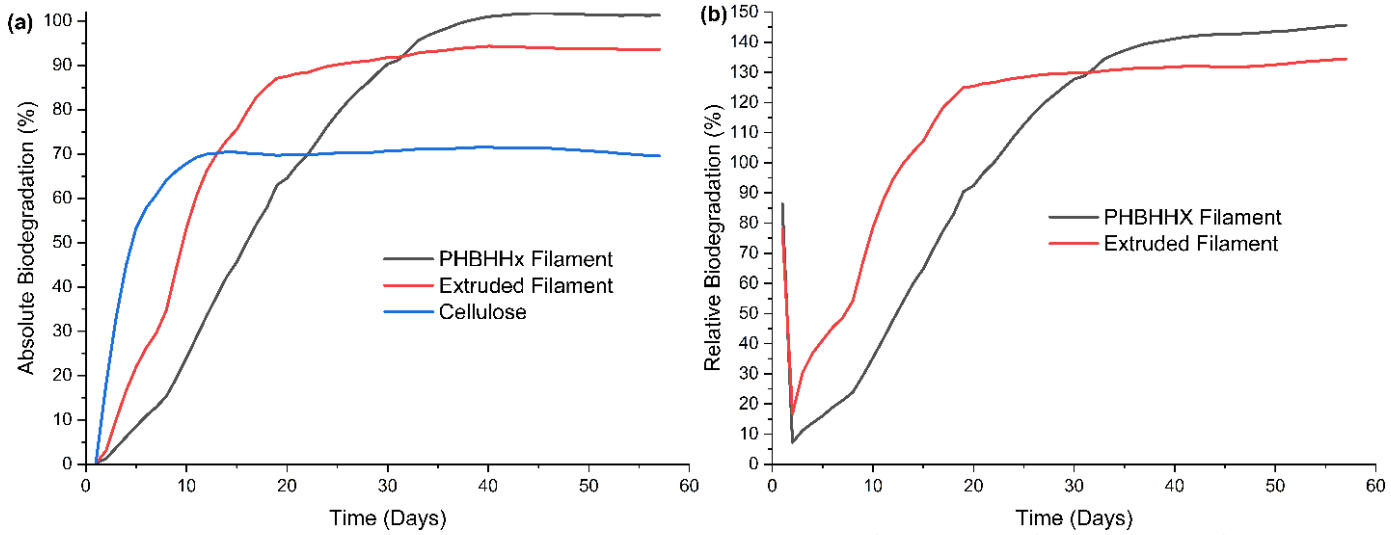

Figure 5. (a) Absolute Biodegradation percentages and 5 (b) relative biodegradation percentages of PHBHHx-based filament before and after 3D print nozzle extrusion under respirometry conditions.

Disintegration results in industrial composting conditions corroborated respirometry, with filament and extrudate samples being visually undetectable to the unaided eye by 7 and 2 weeks, respectively (**Figure 6, S2-S3**). An increase in sample mass between initial values and week 1 is due to the acquisition of dirt and water from the disintegration medium during disintegration testing.

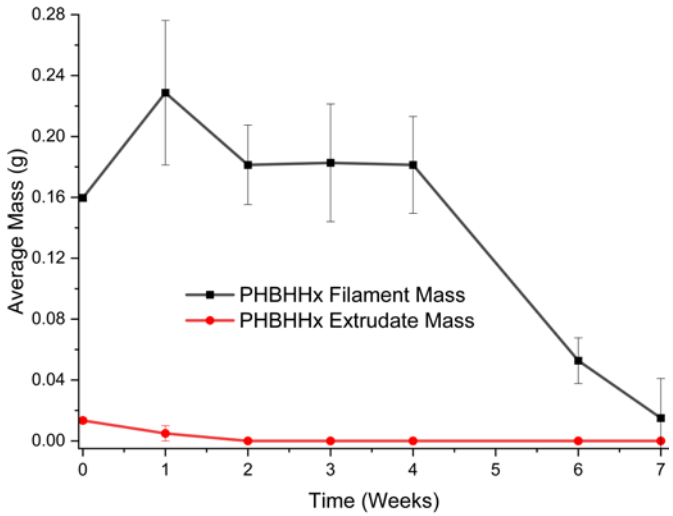

Figure 6. Disintegration sample masses over time for PHBHHx-based filament and extrudate. All data points represent averages of three replicates (n=3). Error bars denote standard deviations of three replicates.

To prevent interruption of bacterial colonization during disintegration photography, samples were handled carefully to prevent disturbance of adhered substrate and microbial colonies. Masses were instead taken as an aggregate of the test sample and its adherents. This data confirms that NMI filament disintegrates rapidly in industrial compost conditions. Automated Raman microscopy experiments analyzed a random sample of 5019 and 9794 particles from the filament and extrudate degradation residues respectively, and no PHBHHx microplastics larger than 10 microns were detected for either the NMI filament or the extrudate in the industrial compost after 57 days (**Figure S4-S7, Table S4**).

Under the conditions of the toxicity test, the survivability of the earthworm *E. fetida* was no different from the blank controls when exposed to either 4,300 or 48,000 ppm of NMI filament (dry weight basis). The toxicity limits and LC50 were not determined from these concentrations and the results of the study are presented in **Table S5**. Overall, these results indicate that the NMI filament was non-toxic to *E. fetida*. Therefore, the collective microbial catabolism (respirometry), disintegration, Raman microscopy and toxicology testing document that NMI filament meets the Bioseniatic™ standard.

Comparison of print masses enables quantification of 3D printing waste potentially offset by PHBHHx-based biodegradable feedstock. The masses of PLA, photocurable, and NMI filament resins in each print are tabulated in (**Table 3**). The masses of the NMI filament prints were all lower than their PLA counterparts due to a lower density of the PHA material (1.21g/mL vs. 1.24g/mL of PLA) and lower than the SLA prints due to the SLA slicing method, which generated a platform of material that holds the desired part and its support structures off of the metal build plate, but which ultimately becomes discarded waste. Overall, printing these four anatomical models with NMI filament, as opposed to the usual feedstocks, could have prevented 312.64 grams of total micronized plastic waste, a portion of which would have afforded no direct value to the use of the printed objects. The utilization of biologically degradable 3D printing feedstocks has the potential to prevent the production of pollutants while

still providing a high-level of print resolution. A literature search did not identify a scrupulous evaluation of the waste generated from the 3D printing industry. However, a recent report from *Filamentive* describes an estimated 33% wastage of filament by mass due to print failures and discarded objects, leading to approximately 379,000 kilograms in environmentally persistent plastic waste per year in the United Kingdom alone (Toor 2023). This, coupled with the fact that any print that is not a durable good will also eventually be discarded, leads us to reason that all FDM filament mass becomes waste and therefore using biologically degradable alternatives for as many FDM printing applications as possible would substantially reduce the quantity of environmentally persistent plastics generated by FDM printing.

Table 3. Print mass comparison between standard printing materials and PHBHHx-based filament.

Print	**Mass** (PLA, grams)	**Mass** (SLA Resin, grams)	**Mass** (*PHBHHx*, grams)
Cat Skull	227.0	--	221.5
Aorta	81.9	--	79.9
Vertebra 1	--	1.85	0.98
Vertebra 2	--	1.89	1.96

Conclusions

A PHBHHx-based alternative feedstock for FDM 3D printing of anatomical models was examined for its precision and biological degradation. Both small and medium scale prints that had previously been printed using non-biologically degradable filament were successfully recreated using the NMI filament, showing comparable surface quality compared to conventional materials. Print parameter tuning afforded high-quality prints at both small and medium scale. Both the as-supplied NMI filament and extrudates from the 3D printing nozzle degraded rapidly in industrial compost conditions and were visibly disintegrated in under two months. Raman microscopy revealed that the degraded filament did not form micronized particles larger than 10 microns, and an earthworm toxicity study showed the degrading filament was not toxic to *E. fetida*. Biologically degradable NMI filament has the potential to reduce the global plastic pollution problem by replacing, when feasible, environmentally persistent FDM in the 3D printing industry. The filament used in this study is expected to be commercially available in early 2024.

Acknowledgements

This work was funded in part by a grant from the RWDC Environmental Stewardship Foundation. The authors would like to especially thank Ryan Skinner for his foresight in understanding the need for biologically degradable 3D printing formulations and in challenging us to use our expertise and extensive repertoire of PHA polymers to formulate Bioseniatic™ 3D printing filament and resins.

References

Chen, G. Q. 2010. Plastics Completely Synthesized by Bacteria: Polyhydroxyalkanoates. In: Chen, GQ. (eds) Plastics from Bacteria. Microbiology Monographs, vol 14. Springer, Berlin, Heidelberg. 17-37.

Crump, S. S. 1992. Apparatus and method for creating three-dimensional objects. U.S. Patent No. 5,121,329.

George, E., Liacouras, P., Rybicki, F. J., and Mitsouras, D. 2017. Measuring and establishing the accuracy and reproducibility of 3D printed medical models. *Radiographics* 37(5):1424-1450.

Gregory, D. A., Fricker, A., Mitrev, P., Ray, M., Asare, E., Sim, D., Larpnimitchai, S., Zhang, Z., Ma, J., and Tetali, S. 2023. Additive Manufacturing of Polyhydroxyalkanoate-Based Blends Using Fused Deposition Modelling for the Development of Biomedical Devices. *Journal of Functional Biomaterials.* 14 (1):40.

Kovalcik, A., Sangroniz, L., Kalina, M., Skopalova, K., Humpolíček, P., Omastova, M., Mundigler, N., and Müller, A. J. 2020. Properties of scaffolds prepared by fused deposition modeling of poly (hydroxyalkanoates). *International Journal of Biological Macromolecules.* 161:364-376.

Lavers, J. L., Hutton, I., and Bond, A. L. 2019. Clinical Pathology of Plastic Ingestion in Marine Birds and Relationships with Blood Chemistry. *Environ Sci Technol.* 53(15):9224-9231.

Low, C. M., Morris, J. M., Matsumoto, J. S., Stokken, J. K., O'Brien, E. K., and Choby, G. 2019. Use of 3D-printed and 2D-illustrated international frontal sinus anatomy classification anatomic models for resident education. *Otolaryngology–Head and Neck Surgery.* 161(4):705-713.

Mehrpouya, M., Vahabi, H., Barletta, M., Laheurte, P., and Langlois, V. 2021. Additive manufacturing of polyhydroxyalkanoates (PHAs) biopolymers: Materials, printing techniques, and applications. *Materials Science and Engineering.* 127:112216.

Paul, G. M., Rezaienia, A., Wen, P., Condoor, S., Parkar, N., King, W., and Korakianitis, T. 2018. Medical applications for 3D printing: recent developments. *Mo Med*. 115(1):75-81.

Qu, X., Qiong W., Liang, J., Qu, X., Wang, S., and Chen, G. 2005. Enhanced vascular-related cellular affinity on surface modified copolyesters of 3-hydroxybutyrate and 3-hydroxyhexanoate (PHBHHx). *Biomaterials.* 26(34): 6991-7001.

Ritchie, B. W. 2022. Plasticosis: Is it a ticking health bomb? International Ornithologists' Union Webinar Series, https://www.internationalornithology.org/iou-webinar-series.

Rodríguez-Hernández, A. G., Chiodoni, A., Bocchini, S., and Vazquez-Duhalt, R. 2020. 3D printer waste, a new source of nanoplastic pollutants. *Environ Pollut.* 267:115609.

Squelch, A. 2018. 3D printing and medical imaging. *J Med Radiat Sci.* 65(3):171-172.

Toor, R. 2023. How Much Plastic Waste does 3D Printing Really Generate? Filamentive. Accessed 29 June 2023. https://www.filamentive.com/how-much-plastic-waste-does-3d-printing-really-generate/

University of Georgia. n.d. "Bioseniatic™ (bi-ō-sē-nē-a-tik) criteria." University of Georgia. Accessed 27 September 2023. https://newmaterials.uga.edu/bioseniatic-criteria/

White, E. M., Clark, S., Manire, C. A., Crawford, B., Wang, S., Locklin J., and Ritchie, B. W. 2018. Ingested Micronizing Plastic Particle Compositions and Size Distributions within Stranded Post-Hatchling Sea Turtles. *Environ Sci Technol.* 52(18):10307-10316.

Yap, Y. L., Tan, E. Y. S., Tan, J. H. K., Peh, Z. K., Low, X. Y., Yeong, W. Y., and Laude, A. 2017. 3D printed bio-models for medical applications. *Rapid Prototyping Journal*. 23(2), 227-235.

Authors

Joshua C. Bledsoe, BSc is a PhD candidate in organic chemistry at the University of Georgia Franklin College of Arts and Sciences, in the Department of Chemistry. He is conducting research with the UGA New Materials Institute.

Brad E. Gilleland, MS is a medical illustrator in the Educational Resources Center at the UGA College of Veterinary Medicine.

Austin F. Wright, BSc is a research professional at the UGA New Materials Institute.

Evan M. White, PhD is the director of the Bioseniatic℠ Laboratory at the UGA New Materials Institute.

Grant H. Crane, PhD is a postdoctoral researcher at the UGA New Materials Institute.

Christopher B. Herron, BFA is the digital media coordinator for the Educational Resources Center at the UGA College of Veterinary Medicine.

Jason J. Locklin, PhD is the director of the UGA New Materials Institute and a professor of chemistry at UGA.

Branson W. Ritchie, PhD, DVM is the director of technological development and implementation at the UGA New Materials Institute and a professor based in the Department of Small Animal Medicine and Surgery at UGA. britchie@uga.edu

Licensing